Freely Flowing Currents and Electric Field Expulsion in Viscous Electronics

Michal Shavit,[1] Andrey Shytov,[2] and Gregory Falkovich[1,3,4]
[1]Weizmann Institute of Science, Rehovot 76100 Israel
[2]University of Exeter, Stocker Road, Exeter EX4 4QL, United Kingdom
[3]Novosibirsk State University, Novosibirsk 630090, Russia
[4]Institute for Information Transmission Problems, Moscow 127051, Russia

(Received 2 January 2019; published 9 July 2019)

Electronic fluids bring into hydrodynamics a new setting: equipotential flow sources embedded inside the fluid. Here we show that the nonlocal relation between the current and electric field due to momentum-conserving interparticle collisions leads to a total or partial field expulsion from such flows. That results in freely flowing currents in the bulk and a boundary jump in the electric potential at current-injecting electrodes. We derive a new type of boundary conditions, appropriate for the case. We then analyze current distribution in free flows, discuss how the field expulsion depends upon the geometry of the electrode, and link the phenomenon to the breakdown of conformal invariance.

DOI: 10.1103/PhysRevLett.123.026801

We experience now a rare moment of intense interaction between the fields of solids and fluids. This is due to the appearance of new high-mobility materials where current carriers exchange momentum faster than lose it to the lattice, so that their collective motion is a viscous fluid flow [1–14]. Ideas from fluid mechanics can solve problems of nanoscale electronics: in particular, decrease resistance below the ballistic limit and make the current flow against the electric field [10,15–17]. As we show here, no less remarkable is what electronics can do for fluid mechanics: 150 years after Stokes, it can reveal new fundamental phenomena in laminar flows, never predicted or observed before. The reason is that electronics brings a new setting not regularly considered in low-Reynolds hydrodynamics—equipotential (metallic) electrodes serving as flow sources embedded inside the fluid. We show below that the conditions on the electric potential (pressure) imposed by sources could be in conflict with those of a viscous flow, which leads to anomalies at the boundaries and novel flow properties; see Fig. 1.

Electronic fluids (e fluids) are characterized by an unusual response of the electric current to electric field $\mathbf{E}$. Instead of the usual Ohm's law, $ne\mathbf{v} = \sigma\mathbf{E}$, charge flows at the scales exceeding the electron-electron (e-e) mean free path l_{ee} are described by the combined Ohm-Stokes equation, stating that the electric field must now overcome both Ohmic and viscous friction:

$$(\eta\Delta - n^2e^2/\sigma)\mathbf{v} = -ne\mathbf{E}. \tag{1}$$

Here n, e, and $\mathbf{v}$ are the number carrier density, charge, and mean velocity, respectively, and σ is the medium conductivity. The nonlocal first term in (1) represents momentum diffusion due to momentum-conserving scattering between carriers and is proportional to the viscosity η.

The simultaneous action of momentum loss and diffusion described by (1) leads to phenomena novel for both hydrodynamics and electronics. Consider an incompressible flow, $\nabla\cdot\mathbf{v} = 0$, and a potential field: $\mathbf{E} = -\nabla\phi$. In that case, solving Eq. (1) appears deceptively simple: Any solution with $\eta = 0$ (purely Ohmic flow) also provides a solution for $\eta \neq 0$, since the viscous force vanishes identically: $\Delta\mathbf{v} \propto \nabla\Delta\phi = 0$. This suggests a paradoxical conclusion: The flow pattern $\mathbf{v}(\mathbf{r})$ is not affected by viscous

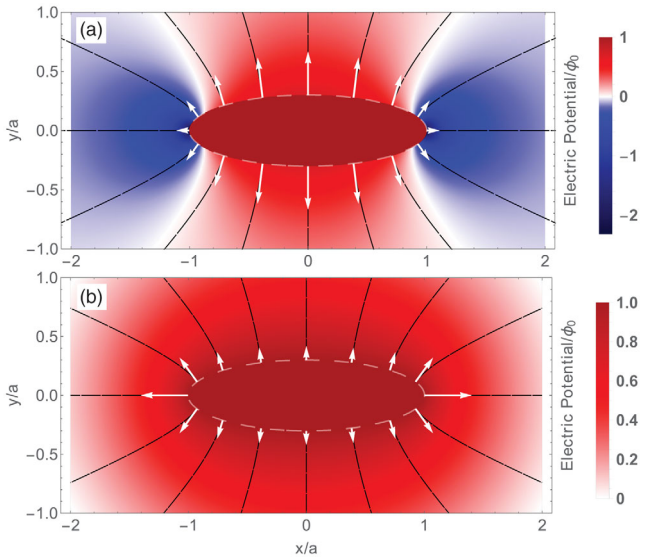

FIG. 1. Streamlines (black), velocity (white arrows), and potential color map for current from an elliptic source ($b = 0.3a$) in (a) viscous and (b) Ohmic regimes. The current near the tips is enhanced for the Ohmic and suppressed for the viscous flow. Viscous drag near the tips results in a negative voltage whose magnitude exceeds the driving voltage.

friction, and the electric field driving the flow vanishes in the purely viscous limit $\sigma \to \infty$.

Vanishing of the viscous force, however counterintuitive, can be verified explicitly in the simplest case of a spherical electrode ejecting a radial current. The velocity field is readily obtained from current conservation:

$$ne\mathbf{v}(\mathbf{r}) = I\mathbf{e}_r/\Omega_d r^{d-1}. \tag{2}$$

Here r is the distance to the source center, I is the total current, and Ω_d is the area of a unit sphere in d dimensions. Since $\mathbf{v}$ is a gradient of a harmonic function, the viscous force $\Delta\mathbf{v}$ vanishes everywhere (this remains true if one adds uniform circulation, for instance, $v_\theta \propto 1/r$ in 2d). The electric field outside is indeed independent of viscosity: $\nabla\phi = I\mathbf{e}_r/\Omega_d r^{d-1}\sigma$. We therefore conclude that an electric field is not required within the system bulk to drive a purely viscous flow, i.e., when $\sigma = \infty$. Yet the paradox remains: The viscous stress tensor $\sigma_{ij} = \eta(\partial_j v_i + \partial_i v_j)$ is nonzero as well as the energy dissipation rate due to viscous friction,

$$P = \frac{1}{2\eta}\int \sum_{i,j} (\sigma_{ij})^2 dV > 0. \tag{3}$$

In other words, even though the net viscous force (divergence of the stress tensor) acting on any fluid element is zero, there are nonzero forces acting on the opposite sides of the element and deforming it, which must lead to dissipation. The energy loss P in the bulk must be compensated by the work $\phi_0 I$ performed by the current source. This requires a finite electrode potential relative to sink at infinity: $\phi_0 = P/I = 2\eta(d-1)I/(ne)^2\Omega_d a^d$ (a is the electrode radius). The contribution of the infinite viscous medium to the total resistance of the system is thus determined by the electrode size: $R = \phi_0/I = 2\eta(d-1)/(ne)^2\Omega_d a^d$. To reconcile finite ϕ_0 with vanishing $\phi(\mathbf{r})$ in the bulk, we conclude that the potential distribution must exhibit a sharp viscosity-dependent drop across a thin Knudsen layer of thickness $\sim l_{ee}$, where the Stokes equation is not applicable. Note that the jump of the potential (pressure) at the boundary gives the momentum flux $(ne)\phi_0$, which is exactly equal to the normal component of the viscous stress tensor, $\sigma_{nn} = -2\eta\partial_r v_r$. In other words, the potential discontinuity can be paraphrased as the continuity of the normal flux of normal momentum. Indeed, viscous stresses are absent inside the electrode but present outside, so that the potential jump compensates the jump in the stress. That potential jump is similar to the Kapitza temperature jump upon heat transfer through a solid-liquid interface [18].

The electric field is thus expelled from the bulk and is concentrated in the boundary layer in a viscous flow. Potential jump is proportional to the viscosity, that is to the mean free path. That means that the electric field inside the ballistic layer is independent of the mean free path. When one goes deep into the hydrodynamic regime (say, by increasing the temperature in graphene), the mean free path shrinks but the electric field stays finite.

Stokes encountered a similar phenomenon of bulk dissipation equal to the surface work in his analysis of the decay of water waves: The flow in the bulk is potential, while the viscous forces only perform work on the surface [19]; see also [20].

The expulsion of the field from the bulk and its concentration at microscopic scales can be verified by analyzing the kinetics of momentum-conserving $e-e$ collisions [21,22] for a pointlike electrode, $a \ll l_{ee}$. Neglecting Ohmic momentum losses, such an approach yields a potential that in the ballistic domain $r \ll l_{ee}$ decays slowly: $\phi(\mathbf{r}) \propto 1/r$ in $d = 2$. The potential falls rapidly at large distances, $\phi(\mathbf{r}) \propto \exp(-r/l_{ee})$. In other words, a point source produces a radial flow having a constant potential at $r \gg l_{ee}$. By superposition, this is also true for an arbitrary combination of point sources and sinks. However, field expulsion is only approximate for finite-size sources and sinks, because they impose boundary conditions.

How is the above picture of field expulsion modified for an electrode of an arbitrary shape? A purely Ohmic flow in 2d can be found via conformal mapping that deforms one electrode into another and also transforms streamlines and potential contours. The naive reasoning outlined above suggests that, when viscosity is present, the transformation of the potential might still be possible due to conformal invariance of the Laplacian. Below, we demonstrate that this conformal equivalence does not hold for viscous flows, since the field distribution depends nontrivially upon the shape of the electrode; in particular, for nonsymmetric electrodes the flow, in general, is not potential and the electric field partially penetrates the fluid.

Indeed, to determine the flow, one needs to solve Eq. (1) supplemented with boundary conditions, which must follow from the same variational principle that gives Eq. (1), i.e., minimization of the dissipated energy (3). Let us minimize the dissipation rate $P[\mathbf{v}]$ as a functional of the velocity field $\mathbf{v}(\mathbf{r})$, for a given total current emitted by the electrode. Variation with respect to the bulk velocity gives (1), while variation with respect to the normal velocity on the source confirms the boundary condition (b.c.) in the form of the normal flux continuity (see Supplemental Material [23]):

$$ne[\phi_0 - \phi(\mathbf{r})] = -\sigma_{ij}n_i n_j \equiv \sigma_{nn}, \tag{4}$$

where $\mathbf{n}$ is the unit vector normal to the boundary and $\phi(\mathbf{r})$ is the boundary value of the potential satisfying Eq. (1). The second boundary condition depends on the nature of the interface between the source and the fluid. In particular, one can consider either a momentum-relaxing no-slip interface with $\mathbf{v}_t = \mathbf{v} \times \hat{\mathbf{n}} = 0$ or a smooth no-stress interface with $\sigma_{nt} = 0$. In what follows, we restrict ourselves to the no-slip case for simplicity. In this case, using

incompressibility $\nabla \cdot \mathbf{v} = 0$, one can rewrite (4) via the signed extrinsic curvature K of the boundary:

$$ne[\phi_0 - \phi(\mathbf{r})] = 2\eta K(\mathbf{v} \cdot \hat{\mathbf{n}}). \tag{5}$$

This novel boundary condition is our main technical result and the basis of the subsequent considerations. It can be interpreted as a universal, viscosity-dependent contribution to contact resistance which cannot be ignored for a nonflat electrode. It is remarkable that this contribution can be both positive and negative depending on the curvature sign. Indeed, to balance the viscous stress, the electric field in the ballistic layer is directed along (against) the current for a positive (negative) curvature. For example, consider the viscous flow in an annulus between two concentric circular electrodes of radii r_1 and $r_2 > r_1$, known as the Corbino disk geometry (see Fig. 2). The resistance of such a system is determined by the two potential jumps each given by Eq. (5):

$$R_0 = \eta(r_1^{-2} - r_2^{-2})/\pi(ne)^2. \tag{6}$$

Since the Stokes equation is symmetric under $\mathbf{v} \to -\mathbf{v}$, $\phi \to -\phi$, reversal of the current reverses the jumps.

If the curvature K varies along the interface, the potential $\phi(\mathbf{r})$, in general, is not a constant, which results in a nonvanishing field in the bulk. Therefore, Eq. (4) provides an example of a conformal anomaly in classical physics: Phenomena at microscopic length scale l_{ee} affect the flow at however large distances in a universal way, invalidating conformal invariant solutions to Eq. (1).

To demonstrate explicitly the breakdown of conformal invariance and partial penetration of the field into the flow, we consider an ellipse as the simplest nontrivial source with a variable curvature. We introduce elliptic coordinates ρ, θ:

$$x = \sqrt{a^2 - b^2}\cosh\rho\cos\theta, \qquad y = \sqrt{a^2 - b^2}\sinh\rho\sin\theta,$$

where $a > b$ are the semiaxes, $0 \le \theta \le 2\pi$ is the polar angle, and $\rho \ge \rho_0 = \tanh^{-1}(b/a)$ is the radial variable, $\rho = \rho_0$ at the electrode. This yields orthogonal coordinates in which the scaling factors $h_i = |\partial\mathbf{x}/\partial i|$ are equal: $h_\rho = h_\theta = \sqrt{(a^2 - b^2)(\sinh^2\rho + \sin^2\theta)}$, so that the variables (ρ, θ) are related to (x, y) by a conformal map, which facilitates the calculation of Laplacians. We seek a solution of the Stokes equation, that is, (1) with $\sigma = \infty$, supplied with the b.c. (5) with the curvature $K = (h_\rho h_\theta)^{-1}\partial_\rho h_\theta$. We also assume zero tangential velocity $v_\theta = 0$ at $\rho = \rho_0$, electrode potential ϕ_0, and zero potential at infinity. Interestingly, the velocity field is radial everywhere (the details are in Supplemental Material [23]):

$$\mathbf{v}(\rho, \theta) = \frac{ne\phi_0(a^2 - b^2)}{\eta h_\theta(\rho, \theta)}(\sin^2\theta + \sinh^2\rho_0)\mathbf{e}_\rho. \tag{7}$$

The potential outside the source is nonuniform:

$$\frac{\phi(\rho, \theta)}{\phi_0} = 1 - \frac{\sinh 2\rho}{2(\sin^2\theta + \sinh^2\rho)}, \tag{8}$$

which gives a nonvanishing electrical field inside the viscous domain. At large distances, the potential is a quadrupole proportional to the eccentricity of the ellipse: $\phi(x, y) \propto (a^2 - b^2)(y^2 - x^2)/r^4$. It changes sign on the lines $x = y$, as for a point source in a half-plane [24].

It is instructive to compare the viscous flow (7) to the purely Ohmic flow, $\mathbf{v}_\Omega(\rho, \theta) \propto h_\theta^{-1}\hat{\mathbf{e}}_\rho$, $\phi_\Omega(\rho, \theta) \propto \rho$, which can be obtained by a conformal deformation of the flow emitted by a circular electrode. The comparison can be seen in Fig. 1. The Ohmic flow is also radial, with the current concentrated near the tips $\theta = 0, \pi$, where the curvature is maximal. In sharp contrast, the viscous current mainly flows from flatter parts, while at the tips it is suppressed by the $\sin^2\theta$ factor in (7). The slow viscous current along the directions around the minimum is dragged by the viscous force from adjacent faster currents. That viscous force is balanced by the electric field directed against the current [17]. The potential jump at the electrode tip, according to (8), is $-\phi_0 a/b$, which for a sufficiently eccentric ellipse can significantly exceed, by absolute magnitude, the driving voltage ϕ_0.

The conformal invariance is indeed broken for nonzero η: The solution for a noncircular electrode cannot be obtained from the flow outside a circular electrode by a conformal map, which gives the potential constant along the electrode surface violating (5). Since (7) satisfies both the no-slip and no-stress boundary conditions on the source, our conclusions here are quite general.

The resistance of the medium depends on the source shape and size. In the elliptic case, one finds from Eq. (7)

$$R = \frac{\phi_0}{I} = \frac{2\eta}{\pi(ne)^2(a^2 + b^2)}. \tag{9}$$

The limit $b \to a$ reproduces the resistance for a circular source $R = \eta/\pi(nea)^2$. Comparing that with the kinetic regime, where $\phi \propto 1/r$, we see that the voltage and resistance grow with decreasing the electrode size as $1/a^2$ for $a \gg l_{ee}$ and as $1/a$ for $a \ll l_{ee}$, according to the general relation between viscous and ballistic regimes [17,24]. The resistance of a flat electrode, $b \ll a$, is determined by its width a: $R = 2\eta/\pi(nea)^2$.

The Stokes equation together with the charge continuity relates $\mathbf{E}$ to vorticity $\omega \equiv \nabla \times \mathbf{v}$ of the flow: $ne\mathbf{E} = \eta\nabla \times \omega$. Hence, penetration of the electric field into the fluid makes the flow nonpotential. One can quantify the degree of field expulsion by the dimensionless parameter $\xi \equiv 1 - \eta\int \omega^2 dV/P$, $0 \le \xi \le 1$, so that work $\xi e\phi_0$ is performed per each particle crossing the Knudsen layer. For an elliptic source, ξ takes a particularly transparent form: $\xi = 2ab/(a^2 + b^2)$. In particular, $\xi = 1$ for a circular

source, $b = a$, when the field is fully expelled from the fluid, and $\xi = 0$ for a flat source, $b \ll a$, when the potential jump vanishes according to (5).

So far, we considered vorticity generated by a nonuniform current through the electrode boundary with a nonuniform curvature. Vorticity can be also generated by nonpotential forces, such as the Lorentz or Coriolis force. Applying magnetic field B results in B-dependent velocity and induces an electric field in the bulk already in the circularly symmetric geometry. Consider the above Corbino geometry with two concentric electrodes. Adding B, we account only for the Lorentz force and disregard Hall viscosity assuming large enough scales [25,26]. The Lorentz force gives rise to an angular velocity and vorticity and generates the electric field in the bulk. The force acting on the angular current affects the potential drop and the resistance:

$$R(B) = R_0 + \frac{B^2 r_2^2}{16\pi\eta}\left(1 - \frac{4\gamma^2 \ln^2\gamma}{(\gamma^2-1)^2}\right), \qquad (10)$$

where R_0 is given by (6) and $\gamma \equiv r_2/r_1$ is the aspect ratio. The second term in the rhs of (10) is the magnetoresistance, which is positive. The magnetoresistance quickly grows with r_2 and is inversely proportional to $\eta \propto l_{ee}$, so that it may easily exceed the boundary contribution as the system goes deeper into the fluidity-dominated regime. Redistribution of the field between the boundary and bulk is characterized by a dimensionless number $\beta \equiv neBr_2^2/\eta$, which is the ratio of Lorentz and viscous forces at the outer rim and determines the number of turns the flow makes between the source and the sink. Figure 2 illustrates the dependence of the field inside the bulk for a varying β and its expulsion at $\beta = 0$.

Note briefly that nonzero Ohmic resistivity always dominates at sufficiently large distances for a zero magnetic field; to see expulsion, we need $l_{ee} \ll a \ll l_*$, where $l_* = \sqrt{\sigma\eta}/ne$ is the Ohmic-to-viscous crossover scale [24]. For the Ohmic-Stokes flow between the concentric electrodes, extra resistance $(2\pi\sigma)^{-1}\log(r_2/r_1)$ is added to (6). The viscous term saturates at $r_2 \to \infty$, while Ohmic resistance slowly grows with increasing r_2 and dominates when $r_1^2 \ln(r_2/r_1) \gg (en)^2/\eta\sigma$.

While both Ohmic and viscous flows are inherently dissipative, there is a dramatic difference in the spatial distribution of the work done to compensate this dissipation. In Ohmic flows, the momentum and the energy losses are locally compensated by an electric field proportional to the current at every point. On the contrary, momentum is diffusively conserved by viscous flows, while the energy is lost everywhere there is a velocity gradient. As we have shown here, the electrical work compensating the viscous energy loss can be partially or even fully done on the flow boundaries. Although we used electronic terminology, all the statements are valid for a general incompressible viscous fluid via the replacement $ne\phi \to p$, with p being the pressure.

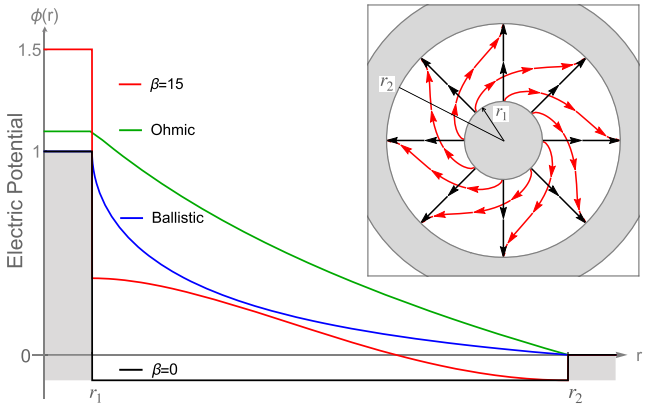

FIG. 2. Potential for a constant current between two concentric circular electrodes, $r_2 = 3r_1$. Different colors indicate different regimes and values of the dimensionless magnetic field β. Black and red correspond to the viscous regime with $\beta = 0$ and $\beta = 15$, respectively, green to the Ohmic regime, where $\phi \propto \log(r_2/r)$, and blue to the ballistic regime, where $\phi \propto \arcsin(r_1/r)$-$\arcsin(r_1/r_2)$. The potential in the viscous regime with and without a magnetic field is quite distinct from those in the Ohmic and ballistic regimes, which makes it amenable to experimental observation. Inset: Streamlines in the viscous regime for $\beta = 0$ (black) and $\beta = 15$ (red).

Let us now discuss a possible experimental observation of the phenomena predicted here for the transition to the viscous regime: field expulsion and increase in magnetoresistance. Distributions of the potential and current described here could be probed, e.g., in graphene via nanoscale imaging methods, such as scanning-gate microscopy [27,28]. The Corbino geometry offers a practical setting where field expulsion can be observed. Indeed, the potential in the viscous regime is dramatically distinct from Ohmic or ballistic (see Fig. 2). Observe that a change of the pattern (upon changing the temperature or concentration) must be possible even when the potential jumps on the electrodes are affected by a nonuniversal contact resistance R_c exceeding the resistance of the medium R (see Supplemental Material [23]). Another observable effect in this geometry must be a sharp increase in magnetoresistance upon passing to the viscous regime. To observe the dramatic difference of the field patterns shown in Fig. 1 including the negative potential, it may be more practical to use needle-shaped electrodes protruding into e fluid from its edge. Most of our findings remain valid for such a setup: Because of (4), the current is redistributed similarly near the tip, and viscous drag results in a strong negative potential. Here, as well, as large R_c affects current uniformly along the contact, "wind shear" near the tip may still induce a negative potential (see Supplemental Material [23]). Finally, the enhancement of viscous effects at the onset of fluidity observed recently [13] suggests that the negative potential near the tip may be maximal in this crossover regime, i.e., when $l_{ee} \sim b$. A detailed analysis of this regime is beyond the scope of this Letter.

In conclusion, we demonstrated how an electric field or pressure gradient can be partially or even completely expelled from viscous flows, so that some or all work compensating viscous dissipation is done on the source. In the electronic setting, when the electrodes are equipotential, the field and the work are concentrated in the surface ballistic layer. In the hydrodynamic setting (say, a vertical tube injecting a fluid between horizontal plates), the pressure gradient and the work are distributed inside the source. Whether the viscous flow is totally or partially force-free depends on the geometry, particularly on the curvature of the source. It is interesting to compare the boundary phenomena described here with those in viscous boundary layers at high Re, such as the velocity slip in the inviscid limits, turbulence, etc.; see, e.g., [20,29].

We are grateful to Leonid Levitov for numerous helpful discussions; his input was indispensable for this work. G. F. thanks Howard Stone for a helpful advice. The work was supported by the Minerva Foundation with funding from the Federal German Ministry for Education and Research, the Israeli Science Foundation, Simons Foundation, the Center for Scientific Excellence, Horizon2020 RISE HALT Consortium, and the Russian Science Foundation Project No. 14-22-00259.

[1] K. Damle and S. Sachdev, Nonzero-temperature transport near quantum critical points, Phys. Rev. B **56**, 8714 (1997).
[2] M. Müller, J. Schmalian, and L. Fritz, Graphene: A Nearly Perfect Fluid, Phys. Rev. Lett. **103**, 025301 (2009).
[3] A. V. Andreev, S. A. Kivelson, and B. Spivak, Hydrodynamic Description of Transport in Strongly Correlated Electron Systems, Phys. Rev. Lett. **106**, 256804 (2011).
[4] D. Forcella, J. Zaanen, D. Valentinis, and D. van der Marel, Electromagnetic properties of viscous charged fluids, Phys. Rev. B **90**, 035143 (2014).
[5] A. Tomadin, G. Vignale, and M. Polini, Corbino Disk Viscometer for 2D Quantum Electron Liquids, Phys. Rev. Lett. **113**, 235901 (2014).
[6] D. E. Sheehy and J. Schmalian, Quantum Critical Scaling in Graphene, Phys. Rev. Lett. **99**, 226803 (2007).
[7] L. Fritz, J. Schmalian, M. Müller, and S. Sachdev, Quantum critical transport in clean graphene, Phys. Rev. B **78**, 085416 (2008).
[8] B. N. Narozhny, I. V. Gornyi, M. Titov, M. Schütt, and A. D. Mirlin, Hydrodynamics in graphene: Linear-response transport, Phys. Rev. B **91**, 035414 (2015).
[9] A. Cortijo, Y. Ferreirós, K. Landsteiner, and M. A. H. Vozmediano, Hall Viscosity from Elastic Gauge Fields in Dirac Crystals, Phys. Rev. Lett. **115**, 177202 (2015).
[10] D. A. Bandurin *et al.*, Negative local resistance caused by viscous electron backflow in graphene, Science **351**, 1055 (2016).
[11] J. Crossno *et al.*, Observation of the Dirac fluid and the breakdown of the Wiedemann-Franz law in graphene, Science **351**, 1058 (2016).
[12] P. J. W. Moll, P. Kushwaha, N. Nandi, B. Schmidt, and A. P. Mackenzie, Evidence for hydrodynamic electron flow in $PdCoO_2$, Science **351**, 1061 (2016).
[13] D. A. Bandurin, A. V. Shytov, L. S. Levitov, R. Krishna Kumar, A. I. Berdyugin, M. Ben Shalom, I. V. Grigorieva, A. K. Geim, and G. Falkovich, Fluidity onset in graphene, Nat. Commun. **9**, 4533 (2018).
[14] A. Lucas, J. Crossno, K. C. Fong, P. Kim, and S. Sachdev, Transport in inhomogeneous quantum critical fluids and in the Dirac fluid in graphene, Phys. Rev. B **93**, 075426 (2016).
[15] H. Guo, E. Ilseven, G. Falkovich, and L. Levitov, Higher-than-ballistic conduction of viscous electron flows, Proc. Natl. Acad. Sci. U.S.A. **114**, 3068 (2017).
[16] R. Krishna Kumar *et al.*, Superballistic flow of viscous electron fluid through graphene constrictions, Nat. Phys. **13**, 1182 (2017).
[17] L. Levitov and G. Falkovich, Electron viscosity, current vortices and negative nonlocal resistance in graphene, Nat. Phys. **12**, 672 (2016).
[18] P. L. Kapitza, Heat transfer and superfluidity of Helium II, Phys. Rev. **60**, 354 (1941).
[19] G. G. Stokes, On the theories of the internal friction of fluids in motion and of the equilibrium and motion of elastic solids, Trans. Cambridge Philos. Soc. **8**, 287 (1845).
[20] G. Falkovich, *Fluid Mechanics* (Cambridge University Press, Cambridge, England, 2018).
[21] H. Guo, E. Ilseven, G. Falkovich, and L. S. Levitov, Higher-than-ballistic conduction of viscous electron flows, Proc. Natl. Acad. Sci. U.S.A. **114**, 3068 (2017).
[22] A. Shytov, J. F. Kong, G. Falkovich, and L. Levitov, Electron Collisions and Negative Nonlocal Response of Ballistic Electrons, Phys. Rev. Lett. **121**, 176805 (2018).
[23] See Supplemental Material at http://link.aps.org/supplemental/10.1103/PhysRevLett.123.026801 for the derivation of boundary conditions as well as a discussion of the validity of our solution to realistic electrode geometries. Derivation of analytical solutions to the Stokes equation in different geometries, including a magnetic field is provided. The connection between field expulsion and conformal invariance is discussed.
[24] G. Falkovich and L. Levitov, Linking Spatial Distributions of Potential and Current in Viscous Electronics, Phys. Rev. Lett. **119**, 066601 (2017).
[25] T. Scaffidi, N. Nandi, B. Schmidt, A. P. Mackenzie, and J. E. Moore, Hydrodynamic Electron Flow and Hall Viscosity, Phys. Rev. Lett. **118**, 226601 (2017).
[26] A. I. Berdyugin *et al.*, Measuring Hall viscosity of graphene's electron fluid, Science **364**, 162 (2019).
[27] B. A. Braem, F. M. D. Pellegrino, A. Principi, M. Röösli, S. Hennel, J. V. Koski, M. Berl, W. Dietsche, W. Wegscheider, M. Polini, T. Ihn, and K. Ensslin, Scanning gate microscopy in a viscous electron fluid, Phys. Rev. B **98**, 241304 (2018).
[28] L. Ella, A. Rozen, J. Birkbeck, M. Ben-Shalom, D. Perello, J. Zultak, T. Taniguchi, K. Watanabe, A. K. Geim, S. Ilani, and J. A. Sulpizio, Simultaneous voltage and current density imaging of flowing electrons in two dimensions, Nat. Nanotechnol. **14**, 480 (2019).
[29] L. Landau and E. Lifshitz, *Fluid Mechanics* (Pergamon, New York, 1959).